Stent with Piezoelectric Transducers for High Spatial Resolution Ultrasound Neuromodulation- a Finite Element Analysis

Dilevicius, Ignas; Serdijn, Wouter A.; Costa, Tiago L.

DOI
10.1109/EMBC48229.2022.9871956

Publication date
2022

Document Version
Final published version

Published in
Proceedings of the 2022 44th Annual International Conference of the IEEE Engineering in Medicine & Biology Society (EMBC)

2022 44th Annual International Conference of
the IEEE Engineering in Medicine & Biology Society (EMBC)
Scottish Event Campus, Glasgow, UK, July 11-15, 2022

Stent with Piezoelectric Transducers for High Spatial Resolution Ultrasound Neuromodulation – a Finite Element Analysis

Ignas Dilevicius, Wouter A. Serdijn, *Fellow, IEEE*, Tiago L. Costa, *Member, IEEE*

***Abstract*— Deep brain stimulation is currently the only technique used in the clinical setting to modulate the neural activity of deep brain nuclei. Recently, low-intensity transcranial focused ultrasound (LIFU) has been shown to reversibly modulate brain activity through a transcranial pathway. Transcranial LIFU requires a low-frequency ultrasound of around 0.5 MHz due to skull attenuation, thus providing poor axial and lateral resolution. This paper proposes a new conceptual device that would use a stent to place a high-frequency ultrasound array within the brain vasculature to achieve high axial and lateral spatial resolution. The first part of this work identified the most commonly treated deep brain nuclei and examined the human brain vasculature for stent placement. Next, a finite element analysis was carried out using a piezoelectric array that follows the blood vessels curvature, and its ability to focus ultrasound waves in clinically relevant brain nuclei was evaluated. The analytical solution provided promising results for deep brain stimulation via a stent with ultrasound transducers for high spatial resolution neuromodulation.**

I. Introduction

Deep brain stimulation (DBS) is currently the only technique used to stimulate deep brain structures in a clinical setting, such as for the treatment of Parkinson's disease (PD) [1]. DBS involves implanting long rigid electrodes into the brain's deep structures, such as the subthalamic nucleus (STN) in PD [1]. The electrodes are wired to an implantable pulse generator (IPG), typically placed subdermally below the clavicle. This electrical stimulation technique provides good spatial resolution (~1 mm) in the immediate vicinity of the electrodes and, most importantly, provides a theoretically unlimited depth of penetration. Nonetheless, the implantation of the electrodes and an IPG requires neurosurgical techniques that are not without risk, such as the occurrence of haemorrhage and infection [1]. Recently, transcranial low-intensity transcranial focused ultrasound (LIFU) has been researched as a promising non-invasive alternative to stimulate deep brain regions. By taking advantage of the low attenuation and scattering of ultrasound waves in soft tissue, LIFU achieves high penetration depth and superior spatial resolution when compared to other transcranial stimulation modalities, such as transcranial magnetic stimulation (tMS) and transcranial direct current stimulation (tDCS) [2]. Although the exact mechanisms by which ultrasound leads to neuromodulation are still not perfectly understood, successful LIFU neuromodulation has been demonstrated across different brain regions in both animal models and humans [3]. In human applications of LIFU, the human skull leads to high attenuation, especially for frequencies above 1 MHz.

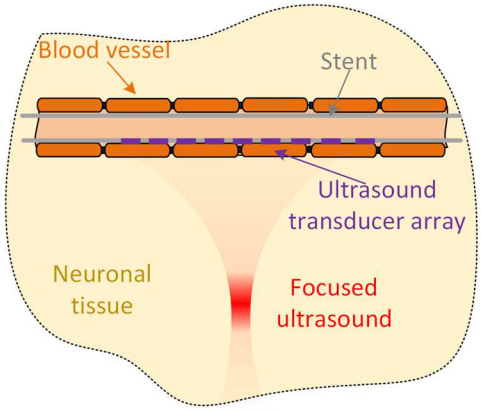

Figure 1. Conceptual brain stimulation device featuring a stent augmented with an ultrasound transducer array for high-spatial resolution neuromodulation

Therefore, a central frequency of 0.5 MHz is typically used, translating into a lateral spatial resolution of around 3 mm and an axial spatial resolution larger than 1 cm [2]. Due to this relatively low frequency, a large aperture transducer is required alongside a coupling device to bridge the gap between transducer and patient. Henceforth, this technique must be performed with an immobilized test subject, preventing its use to treat chronic neurological diseases where either continuous or responsive stimulation is required.

This paper proposes a conceptual device featuring a stent with embedded ultrasound transducers to overcome the spatial resolution limitations and allow continuous stimulation, as illustrated in Figure 1. Neurovascular stents augmented with microelectrode arrays have recently been developed to stimulate and record from cortical circuits in a minimally invasive manner [4] and prolonged safety [5]. However, this approach can only interface with neuronal tissue in the immediate vicinity of the stent. Leveraging on recent developments in miniaturization of ultrasound transducer transmitter arrays and electronics [6-9], and on the developments in the field of Intravascular Ultrasound Imaging (IVUS) [10]. We hypothesise that by augmenting a stent with ultrasound transducer arrays operating at frequencies up to 5 MHz, ultrasound waves with neuromodulatory intensities can be focused with high spatial resolution several centimeters away from the stent. In this paper, the finite element simulation software COMSOL Multiphysics [11] is used to analyse the feasibility of this conceptual device, using the STN as stimulation target in the context of PD.

Ignas Dilevicius (I.Dilevicius@student.tudelft.nl), Wouter Serdijn (W.A.Serdijn@tudelft.nl) and Tiago L. Costa (+31 152789504, T.M.L.daCosta@tudelft.nl) are with the Microelectronics department, Faculty of Electrical Engineering, Mathematics and Computer Science, Delft University of Technology, 2628 CD, Delft, Netherlands

II. Methodology

A. Neurovasculature and stimulation target

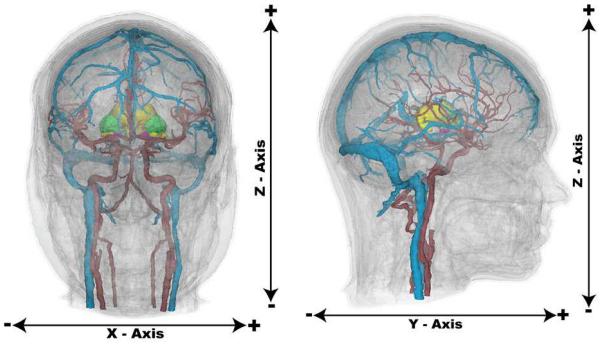

Figure 3 - Multimodal imaging-based detailed anatomical (MIDA) model [11].

The subthalamic nucleus is the most common brain nuclei used in the treatment of Parkinson's disease with DBS [1]. The STN was used to evaluate the feasibility of neuromodulation by focused ultrasound via a nearby blood vessel. A multimodal imaging-based detailed anatomical (MIDA) model of the human head and neck (see Figure 3) was used to visualize the brain vasculature surrounding the STN [12]. The STN model was obtained from [13], and its coordinates within the MIDAM model were determined by locating the mid-commissure point (MCP). The MIDA model was imported as segmentations into the 3D slicer software [14] A central line was drawn between the commissure anterior (CA) and commissure posterior (CP). From the MCP, the STN center of mass was located at ±11.7 mm (X-axis), -2.4 mm (Y-axis) and -6.1 mm (Z-axis).

To identify the suitable blood vessels for an ultrasound array stent, four vascular parameters were chosen; inner diameter, shape, orientation relative to target, and distance to target. The basal vein of Rosenthal (BVR) was selected with an average diameter of 1.56 mm and a distance of 4.25 mm to the STN [15]. The BVR diameter is compatible with stenting, which can be performed in blood vessels as small as 1.5 mm [16]. The BVR was traced in 3D slicer by marking the center of the cross-sectional area of the vessels every 0.5 mm. The marked points were then imported into Solidworks 2020 as a spline. The target coordinate was created, and the shortest line between the target coordinate and the spline was drawn, as shown in Figure 5. These absolute and relative dimensions were used to design the ultrasound transducer array.

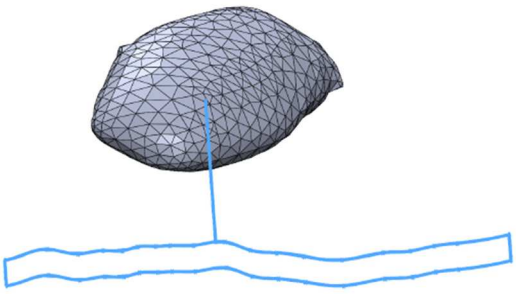

Figure 5 - Targeting the STN via the BVR

Figure 2. Ultrasound array configurations: (a) fully populated 2D array. (b) checkered 2D array

B. Piezoelectric ultrasound transducer array

To simulate the effect of focused ultrasound on the STN originating from a stent inserted in the BVR, an ultrasound transducer array that follows the vessel curvature must be designed. To achieve that, a plane representing the ZX array axis was created by using the target coordinate point, the blood vessel line intersection point and the closest point along the blood vessel. A perpendicular ZY plane was created to the ZX plane between the target coordinate and intersection points. In the ZY plane 100 µm transducers of 262 µm height were sketched with a kerf of 100 µm and extruded by 100 µm. Using the curve driven pattern tool within Solidworks, the extruded transducers were replicated along both directions of the blood vessel with a 100 µm kerf. This type of array will be referred to as a 2D array, as depicted in Figure 2a. To overcome the possible issue of element overlap due to blood vessel curvature, a "checkered" array was designed, as shown in Figure 2b. The array consisted of alternating rows where every other element was removed. Therefore, the array had a 200µm kerf across the array and a 300 µm kerf between the transducers along the array. To simulate the arrays, in COMSOL the "Acoustics-piezoelectric interaction, frequency domain" module was used. The models were imported into COMSOL and a rectangular block was created to engulf the array and its target location with a PML layer of 1 wavelength. PZT-5H material was assigned to the array, and water material properties were assigned to the rest of the domains, as illustrated in Figure 4. Each array element was then assigned a unique coordinate axis for its piezoelectric material and a terminal at the top of the transducer as well as grounded at the bottom. The terminal was set with a sinusoidal voltage with 1 V of amplitude and 5 MHz of frequency. The phase of each driving voltage was calculated to generate a focal spot in a pre-determined location [17]. The calculated Euler transform of piezoelectric material and phase shift for each element were imported to COMSOL. A swept mesh was used for the array with a maximum element size of

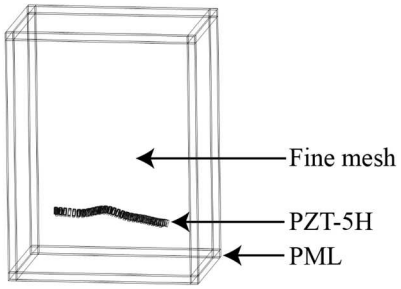

Figure 4. COMSOL Multiphysics model

λ/10, the water domain was meshed using tetrahedral elements with a maximum mesh size of λ/5 and the PML was meshed using a swept mesh with a distribution of 6. The mesh was built in the following order; piezoelectric elements, water domain and PML. Finally, the simulation was carried out using a direct Paradiso solver. The optimal array length for each target region was determined prior to this work using two-dimensional (2D) COMSOL Multiphysics simulations whereas the width of the array was determined by the diameter of the blood vessel.

III. Results & Discussion

Three-dimensional simulations were performed in COMSOL multiphysics of a 2D and a checkered array within the brain vasculature targeting deep brain nuclei. The STN 2D array consisted of 104 (26 x 4) transducers. Whereas, the checkered array consisted 105 ([3 x 2] x 21) transducers. The Comsol simulation results for the 2D and checkered arrays are depicted in Figure 6 and Figure 7, respectively. The checkered array was found to have a lower maximum focal intensity of 0.310 W/cm^2 compared to 0.558 W/cm^2, 44.4% total reduction. Nonetheless, the focal region of full-width half-maximum (FWHM) was significantly smaller of 0.163mm^2 compared to 0.75mm^2, translating into a 78.3% reduction of volume. Furthermore, the checkered array did not experience any significant lobes (Figure 7), whereas, the 2-D array was observed to have lobes along the acoustic path and near the focal region (Figure 6). The STN is around 5.2-13.2 mm in length, 6.4-12.2 mm in width, and around 3.7 mm in depth with a volume ranging from 120-175 mm^3 [18]. The focal region simulated of the 2D array was 2.76 mm by 1.89 mm by 0.2 mm, while the checkered array focal region was found to be 1.82 mm by 0.82 mm by 0.14mm. Henceforth, an ultrasound array within the BVR vasculature should be capable of producing a focal region within the STN, however, as observed with the 2D array the significant lobes would create significant intensity regions outside of the area of interest. A summary of the simulation results is shown in Table I.

Table I - Simulations results for both the 2D and checkered arrays

Parameters	2D	Checkered
# transducers	102	106
Intensity [W/cm2]	0.558	0.31
Focal volume [mm^3]	1.46	0.21

A. Simulation and literature

In this study at 5 MHz the spatial peak intensity and absolute pressures were found to be 0.558 W/cm^2 or 0.140 MPa for a 2D array and 0.311 W/cm^2 or 0.101 MPa for the checkered array. Study by [19] used spatial peak pulse average intensities (I_{SPPA}) of 0.26-0.46 W/cm^2 at 5 MHz to successfully activate the brain circuits in mice. Similarly, [20] found success using I_{SPPA} of 0.54 W/cm^2 at 5 MHz. Moreover, [21] used higher intensity of I_{SPPA} 1.028 W/cm^2 at 5 MHz successfully stimulated the motor cortex of mice. Lastly, [22] was successful in neural excitation at 0.93 MPa. Studies using higher frequencies of 27.38 MHz and 8 MHz by [23] and [24] used I_{SPPA} of 0.465 W/cm^2, and 12 and 5.2 W/cm^2, respectively. Studies, using lower frequencies in general used higher intensities or pressures such as 1.76 MPa at 2 MHz by [25] and I_{SPPA} of 34.96 W/cm^2 at 2.32 MHz by[26]. Therefore, assuming a 50% duty cycle [2] to achieve 1 W/cm^2 or 0.93 MPa requires voltage input of 1.9V or 6.64V, respectively for 2D array. Whereas, for the checkered array to achieve the same intensity and pressure would require input of 2.6V or 9.2V, respectively. Current DBS systems use up to 9V [27]. Henceforth, the simulated arrays targeting the STN are theoretically capable of providing sufficient intensity or pressure required to successfully excite neural activity within the brain. Furthermore, the studies mentioned above commonly do not reference if the mentioned intensity or pressure account for the acoustic attenuation of the skulls which would further reduce the aforementioned values and hence the simulated arrays would require lower voltages to achieve successful excitation. Nonetheless, numerical models have been shown to overestimate peak intensities by around 40 % [30]. In general, the simulated results show a promising system, however, this must be followed up by the design and manufacturing of miniaturized ultrasound transmitter arrays and driving electronics, as well as the development of phantom test setups for acoustic experimental characterization. The feasibility of such device is supported

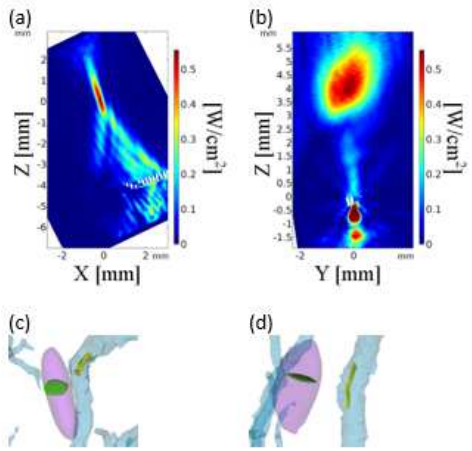

Figure 6 – Focusing ultrasound waves in the STN from the BVR with a 2D array. (a) ZX plane. (b) ZY plane. (c),(d) focal spot (green) inside the STN (purple), with the BVR (blue) featuring the array of transducers (yellow), for ZX and ZY planes, respectively.

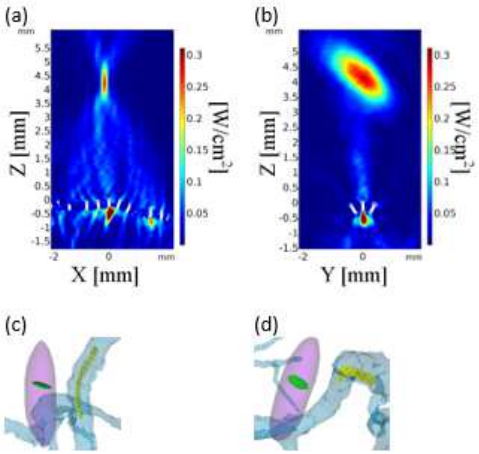

Figure 7 Focusing ultrasound waves in the STN from the BVR with a checkered array. (a) ZX plane. (b) ZY plane. (c),(d) focal spot (green) inside the STN (purple), with the BVR (blue) featuring the array of transducers (yellow), for ZX and ZY planes, respectively.

by the latest developments in the fields of miniaturized ultrasonic systems both for therapeutic and imaging applications, which should be further developed to match the specific constraints of integration in stents.

IV. Conclusion

A minimally invasive stent with an ultrasound array has been proposed for deep brain stimulation allowing the beam profile to bypass the skull and hence use higher frequencies to improve spatial resolution. Three-dimensional FEM simulations were performed in COMSOL multiphysics for a 2-D and checkered array within the BVR targeting the STN. A 104 (2-D 26 x 4) and 105 (Checkered [3 x 2] x 21) transducer arrays within the BVR produced a focal region of full width half intensity within the STN reaching intensities of 0.558 W/cm^2 or 0.140 MPa and 0.311 W/cm^2 or 0.101 MPa, respectively. To achieve neural excitation the 2-D and checkered arrays would require terminal inputs ranging from 1.9-6.6V and 2.6-9.2V, respectively. These values are within the range of currently used DBS systems which use up to 9V. Lastly, a checkered array design was shown as a possible alternative to a 2D array for improved flexibility for blood vessel curvature. Overall, finite element analysis showed that an ultrasound array within the brain vasculature is capable of focusing ultrasound waves with high-spatial resolution in clinically relevant regions of the brain. Hence, stent with an ultrasound array has the potential to be developed as an alternative to deep brain stimulation with high spatial resolution without the need for open brain surgery.

References

[1] A. M. Lozano *et al.*, "Deep brain stimulation: current challenges and future directions," (in eng), *Nat Rev Neurol,* vol. 15, no. 3, pp. 148-160, 2019

[2] J. Blackmore, S. Shrivastava, J. Sallet, C. R. Butler, and R. O. Cleveland, "Ultrasound Neuromodulation: A Review of Results, Mechanisms and Safety," *Ultrasound Med Biol,* vol. 45, no. 7, pp. 1509--1536, 2019

[3] W. J. Tyler, S. W. Lani, and G. M. Hwang, "Ultrasonic modulation of neural circuit activity," *Current Opinion in Neurobiology,* vol. 50, pp. 222--231, 2018

[4] T. J. Oxley *et al.*, "Motor neuroprosthesis implanted with neurointerventional surgery improves capacity for activities of daily living tasks in severe paralysis: first in-human experience," *Journal of NeuroInterventional Surgery,* vol. 13, no. 2, pp. 102-108, 2021

[5] S. A. Raza, N. L. Opie, A. Morokoff, R. P. Sharma, P. J. Mitchell, and T. J. Oxley, "Endovascular Neuromodulation: Safety Profile and Future Directions," *Front Neurol,* vol. 11, 2020

[6] C. Shi *et al.*, "Application of a sub–0.1-mm3 implantable mote for in vivo real-time wireless temperature sensing," *Science Advances,* vol. 7, no. 19, p. eabf6312, 2021

[7] T. Costa, C. Shi, K. Tien, J. Elloian, F. A. Cardoso, and K. Shepard, "An Integrated 2D Ultrasound Phased Array Transmitter in CMOS with Pixel Pitch-Matched Beamforming," *IEEE Transactions on Biomedical Circuits and Systems,* vol. 15, no. 4, pp. 731-742, 2021

[8] C. Shi, T. Costa, J. Elloian, Y. Zhang, and K. L. Shepard, "A 0.065-mm(3) Monolithically-Integrated Ultrasonic Wireless Sensing Mote for Real-Time Physiological Temperature Monitoring," *IEEE Trans Biomed Circuits Syst,* vol. 14, no. 3, pp. 412-424, Jun 2020

[9] C. Shi, T. Costa, J. Elloian, and K. L. Shepard, "Monolithic Integration of Micron-scale Piezoelectric Materials with CMOS for Biomedical Applications," in *2018 IEEE International Electron Devices Meeting (IEDM)*, 1-5 Dec. 2018 2018, pp. 4.5.1-4.5.4, doi: 10.1109/IEDM.2018.8614632.

[10] J. Janjic *et al.*, "A 2-D Ultrasound Transducer With Front-End ASIC and Low Cable Count for 3-D Forward-Looking Intravascular Imaging: Performance and Characterization," *IEEE Trans Ultrason Ferroelectr Freq Control,* vol. 65, no. 10, pp. 1832-1844, Oct 2018

[11] "COMSOL Multiphysics® v. 5.6. www.comsol.com. COMSOL AB, Stockholm, Sweden."

[12] M. I. Iacono *et al.*, "MIDA: A Multimodal Imaging-Based Detailed Anatomical Model of the Human Head and Neck," *PLOS ONE,* vol. 10, no. 4, p. e0124126, 2015

[13] "Neuroimaging Tools and Resources Collaboratory." https://www.nitrc.org/frs/?group_id=1102

[14] A. Fedorov *et al.*, "3D Slicer as an image computing platform for the Quantitative Imaging Network," *Magn Reson Imaging,* vol. 30, no. 9, pp. 1323-41, Nov 2012

[15] C. Deniz, G. Erkan, A. C. U. Berat, and E. Kuyucu Yunus, "Comparative evaluation of dural venous sinuses and cerebral veins using contrast-enhanced spoiled gradient recalled echo and time-of-flight magnetic resonance venography," *J Contemp Med.,* Original Research vol. 9, no. 3, pp. 213-221, 2019

[16] M. J. Price *et al.*, "First Report of the Resolute Onyx 2.0-mm Zotarolimus-Eluting Stent for the Treatment of Coronary Lesions With Very Small Reference Vessel Diameter," *JACC Cardiovasc Interv,* vol. 10, no. 14, pp. 1381-1388, Jul 24 2017

[17] D. H. Turnbull and F. S. Foster, "Beam Steering With Pulsed 2-Dimensional Transducer Arrays," *Ieee Trans. on Ultras. Ferroe. and Frequency Control,* vol. 38, no. 4, pp. 320--333, 1991

[18] I. Mavridis, E. Boviatsis, and S. Anagnostopoulou, "Anatomy of the human subthalamic nucleus: a combined morphometric study," *Anat Res Int,* vol. 2013, p. 319710, 2013

[19] G. F. Li *et al.*, "Improved Anatomical Specificity of Non-invasive Neuro-stimulation by High Frequency (5 MHz) Ultrasound," *Sci Rep,* vol. 6, p. 24738, Apr 20 2016

[20] L. Guofeng *et al.*, "Noninvasive neurostimulation on mice by 5 MHz ultrasound," in *2016 IEEE International Ultrasonics Symposium (IUS)*, 18-21 Sept. 2016 2016, pp. 1-4, doi: 10.1109/ULTSYM.2016.7728592.

[21] S. Kim, H. Kim, C. Shim, and H. J. Lee, "Improved Target Specificity of Transcranial Focused Ultrasound Stimulation (TFUS) using Double-Crossed Ultrasound Transducers," *Annu Int Conf IEEE Eng Med Biol Soc,* vol. 2018, pp. 2679-2682, Jul 2018

[22] G. Li *et al.*, "Imaging-Guided Dual-Target Neuromodulation of the Mouse Brain Using Array Ultrasound," *IEEE Transactions on Ultrasonics, Ferroelectrics, and Frequency Control,* vol. 65, no. 9, pp. 1583-1589, 2018

[23] Z. Lin *et al.*, "Ultrasound Stimulation Modulates Voltage-Gated Potassium Currents Associated With Action Potential Shape in Hippocampal CA1 Pyramidal Neurons," *Front Pharmacol,* vol. 10, p. 544, 2019

[24] E. Kim, E. Anguluan, S. Youn, J. Kim, J. Y. Hwang, and J. G. Kim, "Non-invasive measurement of hemodynamic change during 8 MHz transcranial focused ultrasound stimulation using near-infrared spectroscopy," *BMC Neurosci,* vol. 20, no. 1, p. 12, Mar 18 2019

[25] C. Aurup, H. A. S. Kamimura, and E. E. Konofagou, "High-Resolution, Focused Ultrasound-Mediated Neuromodulation and Detailed Analysis of Electromyography Characteristics Reveals a High Degree of Spatial Specificity in Elicited Responses in Mice in Vivo," in *2018 IEEE International Ultrasonics Symposium (IUS)*, 22-25 Oct. 2018 2018, pp. 1-4, doi: 10.1109/ULTSYM.2018.8579838.

[26] B. C. Gibson *et al.*, "Increased Excitability Induced in the Primary Motor Cortex by Transcranial Ultrasound Stimulation," *Front Neurol,* vol. 9, p. 1007, 2018

[27] R. Ramasubbu, S. Lang, and Z. H. T. Kiss, "Dosing of Electrical Parameters in Deep Brain Stimulation (DBS) for Intractable Depression: A Review of Clinical Studies," *Front Psychiatry,* vol. 9, p. 302, 2018